

## Design, Synthesis and Molecular Docking Studies of Indolo[2,3-*a*]Acridinol Derivatives

Manisekar Sathiyaseelan,<sup>a</sup> Kannadasan Sathishkumar,<sup>b</sup> Amaladoss Nepolraj,<sup>a@</sup>  
Javid A. Malik<sup>c</sup> and Vasyl Shupeniuk<sup>d</sup>

<sup>a</sup>Department of Chemistry, Annai College of Arts and Science (Affiliated to Bharathidasan University, Trichy), Kumbakonam, Tamilnadu 612503, India

<sup>b</sup>Department of Physics, Annai College of Arts and Science (Affiliated to Bharathidasan University, Trichy), Kumbakonam, Tamilnadu 612503, India

<sup>c</sup>Department of Zoology, Guru Ghasidas Vishwavidyalaya, Bilaspur Chhattisgarh 495001, India

<sup>d</sup>Department of the Environment and Chemical Education, Vasyl Stefanyk Precarpathian National University, Ivano-Frankivsk 76018, Ukraine

@ Corresponding author E-mail: nepolraj@gmail.com

*A study of the synthesis of an indolo[2,3-*a*]acridinol derivative using the Claisen ester condensation reaction resulted in the discovery of inexpensive and user-friendly solvents. Structures of the newly synthesized compounds were characterized by FT-IR, <sup>1</sup>H NMR, <sup>13</sup>C NMR, and HRMS analyses. Docking studies showed a strong affinity of indolo[2,3-*a*]acridinol towards prostate cancer-related proteins. The binding affinity closer to 10 kcal/mol indicated effective binding. Indolo[2,3-*a*]acridinol showed strong binding affinities towards protein androgen receptors such as 1GS4, 1T7R, 2AX8, and 3B66 indicating its potential role in protein kinase inhibition. The programs, AutoDock 4 and AutoDock Vina, and Swiss ADME software were applied to dock the target protein with synthesized compounds.*

**Keywords:** Indoloacridinol, Claisen condensation, androgen receptor, molecular docking.

## Дизайн, синтез и исследования молекулярного докинга производных индоло[2,3-*a*]акридинола

М. Сатьясилан,<sup>a</sup> К. Сатишкумар,<sup>b</sup> А. Неполрадж,<sup>a@</sup> Д. А. Малик,<sup>c</sup> В. Шупенюк<sup>d</sup>

<sup>a</sup>Кафедра химии, Колледж искусств и наук Аннаи (филиал Университета Бхаратидасан, Тричи), Кумбаконам, Тамилнаду 612503, Индия

<sup>b</sup>Кафедра физики, Колледж искусств и наук Аннаи (филиал Университета Бхаратидасан, Тричи), Кумбаконам, Тамилнаду 612503, Индия

<sup>c</sup>Кафедра зоологии, Гуру Гасидас Вишвавидьялая, Биласпур Чхаттисгарх 495 001, Индия

<sup>d</sup>Кафедра экологии и химического образования, Прикарпатский национальный университет им. В. Стефаника, Ивано-Франковск 76018, Украина

@ E-mail: nepolraj@gmail.com

*Выявлены недорогие и наиболее удобные растворители, используемые в синтезе производного индоло[2,3-*a*]акридинола с использованием сложноэфирной конденсации Кляйзена. Структуры вновь синтезированных соединений охарактеризованы методами ИК-Фурье, <sup>1</sup>H, <sup>13</sup>C ЯМР и HRMS спектроскопии. Исследования стыковки показали сильное сродство индоло[2,3-*a*]акридинола к белкам, связанным с раком предстательной железы. Аффинность связывания ближе к 10 ккал/моль указывала на эффективное связывание. Индоло[2,3-*a*]акридинол показал сильную аффинность связывания с белковыми андрогенными рецепторами, такими как 1GS4, 1T7R, 2AX8 и 3B66, что указывает на его потенциальную роль в ингибировании протеинкиназы. Для стыковки целевого белка с синтезированными соединениями применяли программы AutoDock 4 и AutoDock Vina, а также программу Swiss ADME.*

**Ключевые слова:** Индолоакридинол, конденсация Кляйзена, андрогенный рецептор, молекулярный докинг.

## Introduction

The main type of nuclear receptor that is activated by contacting any of the androgenic hormones is the androgen receptor (AR), also known as NR3C4 (nuclear receptor subfamily 3, group C, member 4).<sup>[1]</sup> The androgen receptor (AR) is a key target for the development of new anticancer drugs that inhibit cancer cells, mainly castration-resistant prostate cancer (CRPC). When cells in the prostate gland begin to grow out of control, the prostate forms a tumor.<sup>[2]</sup> The prostate gland is exclusively present in men. The prostate is located below the bladder (the hollow organ where urine is kept) and in front of the rectum, and it produces some fluid that is part of the sperm (the last part of the intestines). Seminal glands are located just behind the prostate.<sup>[3,4]</sup>

Cancer disease is a serious public health issue worldwide.<sup>[5,6]</sup> There is a limited number of anticancer drugs on the market. It may be inferred that novel anticancer medicines are urgently needed, as is the finding of appropriate cellular targets for successful cancer treatment.<sup>[7]</sup> Topoisomerase 1 (Top1) was discovered to be present constitutively in various cancers. As a result, the continual quest for safer novel chemical entities with significant anticancer action (lymphoma, breast, leukemia, lung, ovarian, and prostate) became a priority.<sup>[8–10]</sup> Many useful efforts have been done on the enhancement heterocyclic moieties based on their structural framework to develop active anticancer medicines targeting androgen receptors.<sup>[11]</sup> Acridine compounds cause tumour cell death and attract DNA intercalates by eliciting a high activation through a mechanism separate from that generated by DNA damage.<sup>[12]</sup> Its numerous biologically important pharmacologically active scaffolds in medicinal chemistry. Camptothecin **I**, dictamine **II**, skimmianine **III**, khaplofoline **IV**, acronycine **V**, and glyfoline **VI** are examples of well-known Top1 inhibitors (Figure 1).

The solvent-free conventional reaction has attracted high use in recent years as an effective platform for a variety of synthetic transformations, surpassing other bases in terms of yield, reaction time, reaction temperature, and moisture tolerance.<sup>[13–16]</sup> The design, synthesis, and biological characterization of 7,12-dihydro-6*H*-indolo[2,3-*a*]acridin-13-ol (**5**) as new AR antagonists are described in this paper.

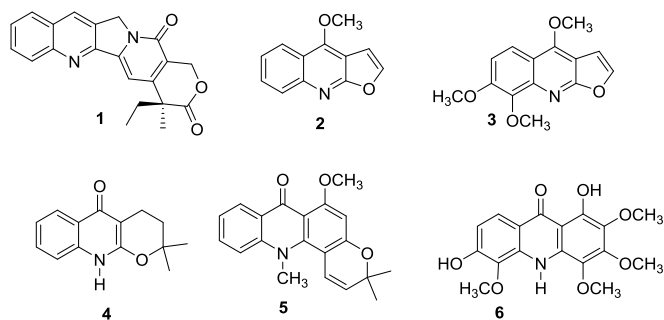


**Figure 1.** Use of some of the established Top1 inhibitors **I–VI**.

## Experimental

### Materials and Methods

All chemicals and solvents are purchased from Fine and Merck Chemicals India. Melting points are uncorrected. Infrared spectral data is recorded using Perkin-Elmer Paragon 1000 FT-IR spectrometer as potassium bromide discs unless otherwise indicated scanning 32 times from 4000 to 400  $\text{cm}^{-1}$  at 4  $\text{cm}^{-1}$  resolution.  $^1\text{H}$  and  $^{13}\text{C}$  NMR spectra are obtained in the  $\text{CDCl}_3$  solvent on a Bruker (400 MHz) instrument.  $^1\text{H}$  NMR data are recorded as follow: chemical shift measured in parts per million (ppm) downfield from TMS (d), multiplicity, observed coupling constant ( $J$ ) in Hertz (Hz), proton count. Multiplicities are reported as singlet (s), broad singlet (br.s), doublet (d), triplet (t), quartet (q), quintet (quin) and multiplet (m).  $^{13}\text{C}$  NMR (100 MHz) chemical shifts are reported in ppm downfield from TMS and identifiable carbons are given. GC-MS information Perkin Elmer, Mass Spectrometer Clarus 600 (EI), Clarus 680 GC is used in the analysis employed a fused silica column, packed with Elite- 5MS (5% biphenyl 95% dimethylpolysiloxane, 30 m  $\times$  0.25 mm ID  $\times$  250  $\mu\text{m}$  df) and the components are separated using helium as carrier gas at a constant flow of 1 mL/min. The injector temperature is set at 260  $^\circ\text{C}$  during the chromatographic run. The 1  $\mu\text{L}$  of extract sample is injected into the instrument the oven temperature is as follows: 60  $^\circ\text{C}$  (2 min); followed by 300  $^\circ\text{C}$  at the rate of 10  $^\circ\text{C min}^{-1}$ ; and 300  $^\circ\text{C}$ , where it is held for 6 min. The mass detector conditions are: transfer line temperature 240  $^\circ\text{C}$ ; ion source temperature 240  $^\circ\text{C}$ ; and ionization mode electron impact at 70eV, a scan time 0.2 sec and scan interval of 0.1 sec. The fragments are ranging from 40 to 600. All compounds are routinely checked by thin layer chromatography (TLC) with Merck silica gel 60 F - 254 glass plates. In column chromatography, Merck silica gel 60-120 mesh, petroleum ether and ethyl acetate, as eluents, are utilized. Solvents and reagents are purified by literature methods. Petroleum ether refers to the hydrocarbon fraction of boiling range 60–80  $^\circ\text{C}$ . Compounds are detected by short and long ultraviolet light and with iodine vapor.

### Synthesis

**9-Hydroxy-3,4-dihydroacridin-1(2*H*)-one (3).** A catalytic amount of sodium hydride was added to an equimolar mixture of methyl 2-aminobenzoate **1** (1.51 mL, 0.1 moles), and cyclohexane-1,3-dione (1.12 g, 0.1 moles). The reaction mixture was then refluxed for 4 hours at 140  $^\circ\text{C}$ . The resulting product was a yellow solid. It was kept at room temperature before being transferred to 500 mL of ice water then neutralized with 10% HCl. The precipitate was filtered out and purified using column chromatography using petroleum ether as the mobile phase and ethyl acetate as the stationary phase (95:05). The product was recrystallized from ethanol to yield a yellow crystalline solid. 2.05 g (80%); FT-IR (KBr)  $\nu_{\text{max}} \text{cm}^{-1}$ : 3363, 3060, 2922, 1703, 1667, 1555, 1300, 1352.  $^1\text{H}$  NMR (500 MHz, DMSO)  $\delta_{\text{H}}$  ppm: 12.93 (bs, 1H, N-H), 7.967 (t, 1H, C7-H), 7.68 (t, 1H, C6-H), 7.42–7.40 (d, 1H, C8-H,  $J = 8$ ), 7.36–7.34 (d, 1H, C5-H  $J = 7$ ), 3.86–3.66 (m, 2H, C3-H), 2.50 (t, 2H, C2-H), 2.18 (t, 2H, C4-H).  $^{13}\text{C}$  NMR (125 MHz, DMSO- $d_6$ )  $\delta_{\text{C}}$  ppm: 199.13, 138.46, 137.90, 132.51, 132.44, 125.14, 123.15, 115.88, 37.05, 30.53, 20.31. GC-MS:  $m/z$  [ $\text{M}^+$ ] 213 (48%).

**7,12-Dihydro-6*H*-indolo[2,3-*a*]acridin-13-ol (5).** A mixture of phenylhydrazine **4** (1.51 g, 0.1 mole) and 9-hydroxy-3,4-dihydroacridin-1(2*H*)-one (**3**) (2.13 g, 0.1 mole) dissolved in 15 mL of acetic acid was refluxed at 140  $^\circ\text{C}$  for 6 hours. The reaction was then monitored via TLC and see where this is progressed. Then the reaction was poured into ice-cold water and purified using a petroleum ether and ethyl acetate mixture in column chromatography (90:10). Yellow crystal, 75 % yield. FT-IR (KBr)  $\nu_{\text{max}} \text{cm}^{-1}$ : 3453, 3228, 3015, 2887, 1617, 1593, 1507.  $^1\text{H}$  NMR (500 MHz,  $\text{CDCl}_3$ )  $\delta_{\text{H}}$  ppm: 11.57 (bs, 1H, indol-N-H), 12.93 (bs, 1H, N-H),

8.00-7.99 (d, 1H, C<sub>12</sub>-H, *J* = 7.5), 7.80-7.77 (d, 1H, C<sub>10</sub>-H), 7.54 (t, 1H, C<sub>9</sub>-H), 7.47 (t, 1H, C<sub>11</sub>-H), 7.34-7.316 (d, 1H, C<sub>4</sub>-H, *J* = 15), 6.69-6.68 (d, 1H, C<sub>1</sub>-H *J* = 8.5), 3.05 (bs, 4H, C<sub>6</sub>-C<sub>7</sub>-H). <sup>13</sup>C NMR (120 MHz, CDCl<sub>3</sub>) δ<sub>c</sub> ppm: 162.74, 154.19, 138.85, 138.07, 136.28, 131.32, 130.41, 129.92, 129.83, 128.28, 128.10, 122.84, 29.70, 20.70. GC-MS: *m/z* [M<sup>+</sup>] 276 (43%).

### ADME analysis

A drug's ability to enter the market is decided not only by its most immediately beneficial potential but also by a good ADME study. Because a wide range of experimental data and high-throughput *in vitro* ADME screens are available, they can predict important properties *in-silico*, which is useful for analyzing the molecules' excellent qualities. This determines which pharmacokinetic parameters, such as ADME, are required under Lipinski's rule. The rule is useful when developing a potential molecule for drug development.<sup>[17]</sup> For the current study, ADME analysis was performed using the SWISS ADME and molinspiration predictor.<sup>[18]</sup> This is a free online server tool for evaluating ADMET features such as water solubility (log*S*), skin permeability (log*K<sub>p</sub>*), synthetic accessibility score (SA), percentage absorption, pharmacokinetics, drug-lead resemblance, and medicinal chemistry friendliness. Importation study of molecules with a molecular weight of 500, 5 hydrogen bond donors (HBD's), 10 hydrogen bond acceptors (HBAs), and 10 rotatable bonds (RBs). The grade analysis result on lipophilicity and hydrophilicity of these compounds was done by combining findings from ILOGP, XLOGP3, WLOGP, ESOL, and SILICOS-IT, which are all log *P* and *S* prediction tools. The aqueous solubility of a compound especially affects its absorption and distribution characteristics, low water solubility often leads to bad absorption, and therefore, the general aim is to avoid poorly soluble compounds. Log*S* is a unit expressing solubility, it is the 10-based logarithm of the solubility measured in mol·L<sup>-1</sup>. The distribution of log*S* between -1 and -4 will be improved for better absorption and distribution of drugs in the body.<sup>[19]</sup>

### Molecular docking

Molecular docking approach in structure-based drug design. The synthesized compound of ligand was drawn with Chem Draw Ultra version 16.0 (Cambridge Software) followed by resulting molecular mechanics (MM2) energy minimization of ligands using ChemBio-3D Ultra version 16.0 with GAMESS Interface by assuring connection error in the bonds. These energy-minimized ligands (structures) MOL, SDF format of that ligands had been converted to mol2 file using open babel and Discovery studio tool and ligand preparation were done using the Chimera software ended up being used in molecular docking study. Crystal structure of human androgen receptor (PDB ID code:1GS4, 1T7R, 2AX8, 3B66)<sup>[20]</sup> was obtained through the Protein Data Bank (<http://www.pdb.org>) and any heteroatoms, water molecules were eliminated for molecular docking studies. Molecular docking was performed utilizing Autodock Tools 1.5.4 package (<http://mgltools.scripps.edu>)<sup>[21]</sup> and Autodock Vina (version 4.2 docking programs) to grasp the drug molecule interaction with protein, the potential binding mode and energy, and analysis the binding affinity of human androgen receptor molecular docking analysis ended up being carried out making use of Autodock 4.2.18. Autodock Vina Wizard approach.<sup>[22]</sup> The synthesized ligand was docked individually against the target protein (PDB ID:1GS4, 1T7R, 2AX8, 3B66). In docked complexes, the ligand conformational poses were keenly observed to obtain useful docking results. The generated docked complexes were evaluated based on the lowest binding energy (kcal/mol) values and structure-activity relationship (SAR) analyses the clear presence of

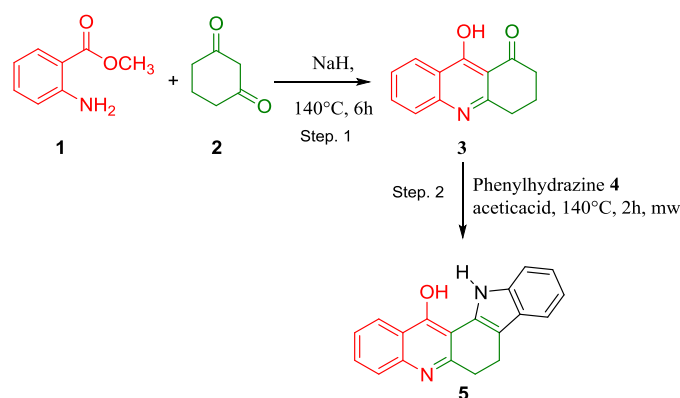
hydrogen bond, hydrophobic interaction between ligand compound, and good control to each focused-on the receptor. The 3D and 2D graphical depictions of all the docked complexes were accomplished by UCSF Chimera 1.10.1, Discovery Studio (2.1.0), PyMOL software, and (<https://proteins.plus/>) online web server.<sup>[23]</sup>

## Results and Discussion

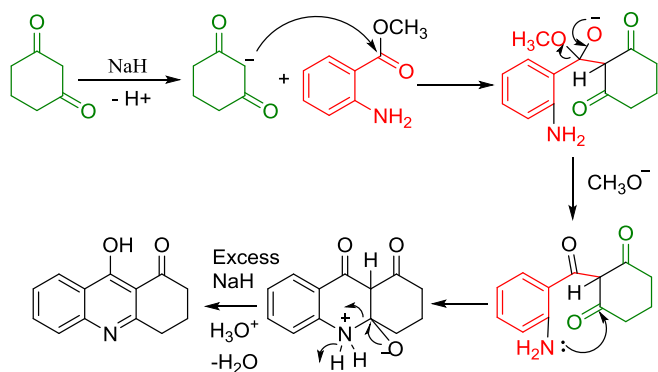
### Chemistry

In the synthetic protocol, the title compound was synthesized in two steps as Fisher-indole (Scheme 1). On equimolar amounts of Claisen ester condensation with 1,3-cyclohexadione **2** using a pinch of sodium hydride, thermal cyclization at high temperature (160 °C) with solvent fewer reaction conditions, methylantharante **1** gave 9-hydroxy-3,4-dihydroacridin-1(2H)-one **3**. In the second stage, phenylhydrazone **4** was condensed with 9-hydroxy-3,4-dihydroacridin-1(2H)-one **3** under Fisher-indole reaction conditions to yield a final compound 7,12-dihydro-6H-indolo[2,3-*a*]acridin-13-ol **5**. The mixture was allowed to stand overnight after the Fisher indole reaction occurs to a strong acid (acetic acid). The total reaction time in the modified Fisher-Indole technique was 1–2 hrs, and no need to stand overnight in the microwave conditions.

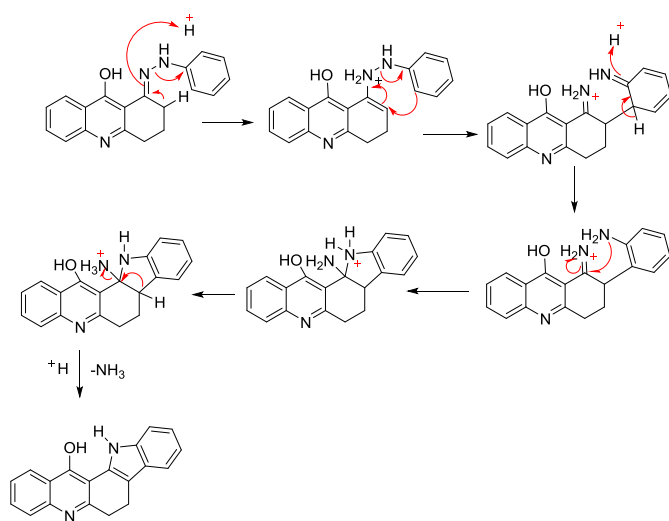
IR spectroscopy and functional group identification were used to confirm the structure of the compounds. To confirm the Claisen product, compound **3** demonstrated the disappearance of the ester group stretching at 1700-1750 cm<sup>-1</sup>, and also the appearance of ketonic carbonyl stretching at 1716 cm<sup>-1</sup> and O-H stretching at 3250 cm<sup>-1</sup>. On methylantharante, a singlet peak representing the OH proton is appeared to be about δ<sub>H</sub> 12.39 ppm, accompanied by a disappearance of three proton singlets at δ<sub>H</sub> 2.50 ppm of OCH<sub>3</sub>, and aromatic protons provided their signals at δ<sub>H</sub> 7.97–7.33 ppm, although 3,4-dihydroacridinone three CH<sub>2</sub> gave their peaks at δ<sub>H</sub> 3.8–2.1 ppm. A signal at δ<sub>C</sub> 199.13 ppm in the <sup>13</sup>C NMR spectra of the compound confirms ketonic carbonyl carbon, and C=N carbon peaks were observed near δ<sub>C</sub> 161.12 ppm. Mass spectra of compound **3** exhibited a molecular ion peak [M<sup>+</sup>] at *m/z* 213 confirming the identity of 9-hydroxy-3,4-dihydroacridin-1(2H)-one.



**Scheme 1.** Synthesis of 7,12-dihydro-6H-indolo[2,3-*a*]acridin-13-ol (**5**).



**Scheme 2:** The possible reaction mechanism is outlined for the synthesis of 9-hydroxy-3,4-dihydroacridin-1(2*H*)-one.



**Scheme 3:** The possible reaction mechanism is outlined for synthesis of 7,12-dihydro-6*H*-indolo[2,3-*a*]acridin-13-ol (**5**).

The absence of ketonic C=O stretching at  $1716\text{ cm}^{-1}$  was seen in the IR spectrum of compound **5**, whereas newly formed OH stretching at  $3453\text{ cm}^{-1}$  confirmed the functional group transformation. The peak value in secondary amine is  $3400\text{ cm}^{-1}$ . Aromatic C–H peaks were shown at  $3000\text{--}3100\text{ cm}^{-1}$ , whereas aliphatic C–H signals were seen at  $2800\text{--}3000\text{ cm}^{-1}$ . Other peaks in this region, like aliphatic and aromatic C–H peaks, overlap. At  $1200\text{--}1300\text{ cm}^{-1}$ , C–N peaks appeared. In  $^1\text{H NMR}$ , a peak representing the NH proton for indole appeared at about  $\delta_{\text{H}} 11.57$ , and an alpha ketonic proton disappeared at  $\delta_{\text{H}} 2.12$ . In  $^{13}\text{C NMR}$  spectrum, C=N carbon peaks were observed near  $\delta_{\text{C}} 160\text{ ppm}$ , and the signals of the ketonic carbon at  $\delta_{\text{C}} 199$  and the aliphatic regional carbon at  $37.05$  disappear. Observing  $m/z 271$  in the mass spectra is important evidence for the availability of 5 moieties; the foregoing data provided a clear input to confirm the molecule as 7,12-dihydro-6*H*-indolo[2,3-*a*]acridin-13-ol.

### ADME Analysis

The predicted chemo-informatic properties had been evaluated by computational tools. *In silico* studies demonstrably suggest that the compound had drug-like prospect properties with no breach of some drug-likeness rules discussed above. It was interesting to see that the results associated with the SWISS ADME and Molinspiration predictor values of  $\log P$ , molar refractivity with the total polar surface area in these molecules were in excellent agreement with the most important rules of drug-likeness. The predicted chemo-informatics properties were evaluated by computational tools. Results exposed that compound 7,12-dihydro-6*H*-indolo[2,3-*a*]acridin-13-ol has the better-predicted value of molecular weight  $286.33\text{ (g/mol)}$  within the range value ( $< 500\text{ g/mol}$ ) which has greater molecular weight compound compared to borderline value. Hydrogen bond acceptor and donor,  $\log P$ , polar surface area ( $\text{\AA}^2$ ), and molar volume ( $\text{\AA}^3$ ) though this compound exhibited a good hydrophilic-lipophilic balance, therefore the same predicted bioavailability, high lipophilicity was expected to show decent GI absorption. In addition,  $48.91\text{ \AA}^2$  value was calculated as the total polar surface area (TPSA), as it is another key property that is related to drug bioavailability. Thus, passively absorbed molecules with  $\text{TPSA} > 140$  are thought to have low oral bioavailability, the molecular polar surface area (PSA) is a very useful parameter for drug transport properties, the molecule is defined as the surface sum over all polar atoms, primarily oxygens, nitrogens, and attached hydrogen atoms. This parameter has been shown to correlate very finely with the human intestinal absorption Caco-2 monolayers permeability and blood-brain barrier penetration. The PSA parameter is commonly used for a drug optimization ability to permeate cells. Prior research data showed the standard value of PSA ( $< 89\text{ \AA}^2$ ).

The Lipinski's rule RO5 of result 0 violation showed that compound **5**, possess good two Hydrogen Bond Accepted and Hydrogen Bond Donor values two,  $\log P 2.42$  which are significantly justified their drug-likeness behavior were justifiable with the standard 7,12-dihydro-6*H*-indolo[2,3-*a*]acridin-13-ol, **5** (pink area reflects the allowed values of drug-likeness properties of the molecule values. The RO5 deviation (Mol. Wt  $\geq 500\text{ g/mol}$ ; HBD  $\geq 5$ ; HBA  $> 10$ ; and  $\log P \geq 5$ ). The drug-likeness score is an amalgam of a complex balance of several molecular properties and structural features which determine the behavior of a molecule as a drug. The drug score is 0.55 good values, which depicted their wonderful drug-like behavior to be androgen receptors. The results got from the Swiss ADME and Molinspiration search engine are listed in Table 1. The boiled-egg diagram analysis shows that the compound is strong within the permissible range of standard drugs, the P-glycoprotein of the CNS system by P-glycoprotein, a point located in boiled eggs yolk is a molecule that passively permeates through the blood-brain barrier (BBB). In the current study, the synthesized ligand and its complexes were initiated to be in a good pact with the criteria and can be said to possess good bioavailability.

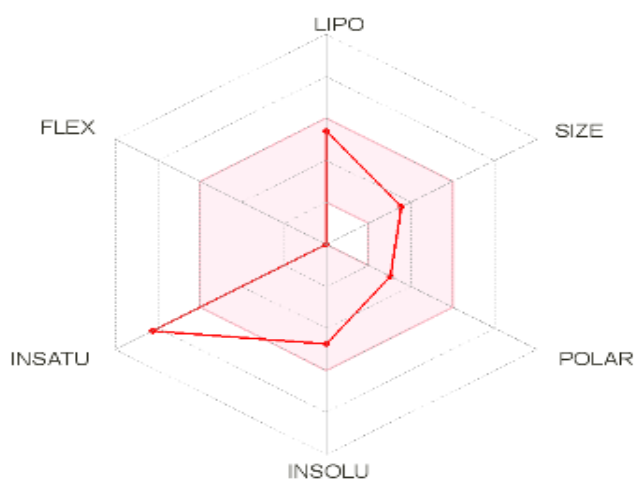


**Figure 2.** Bioavailability radar graph of Synthesis of 7,12-dihydro-6H-indolo[2,3-a]acridin-13-ol (**5**) @ Swiss ADME.

**Table 1.** Physicochemical descriptors and ADME parameters.

M.W, g/mol	286.33
Rotatable bond (RB)	0
Hydrogen bond acceptor (H-A)	2
Hydrogen bond donor (H-D)	2
Topological polar surface area (TPSA)	48.91 Å <sup>2</sup>
MR	88.88
Lipophilicity (W logP)	2.42
Water solubility (ESOL logS)	-4.74
Blood brain-barrier (BBB)	Yes
Permeability coefficient (logK <sub>p</sub> cm <sup>s</sup> <sup>-1</sup> )	-5.24
Lipinski Violations	0
PAINS alerts	0
GI absorption	High
Synthetic accessibility	3.08

#### Molecular docking studies

Autodock vina and Molecular docking studies were performed to find the binding ability of the newly synthesized compound with the crystal structure of the human androgen receptor (PDB ID:1GS4, 1T7R, 2AX8, 3B66). The docking scores of all AR receptors are presented in Table 2 to exhibit good interaction with the AR receptor target proteins. Among all the titled compounds 1GS4 as compared to 1T7R, 2AX8, and 3B66 was found to be most potent and have the highest docking score (−10.1 kcal/mol) from PDB ID.

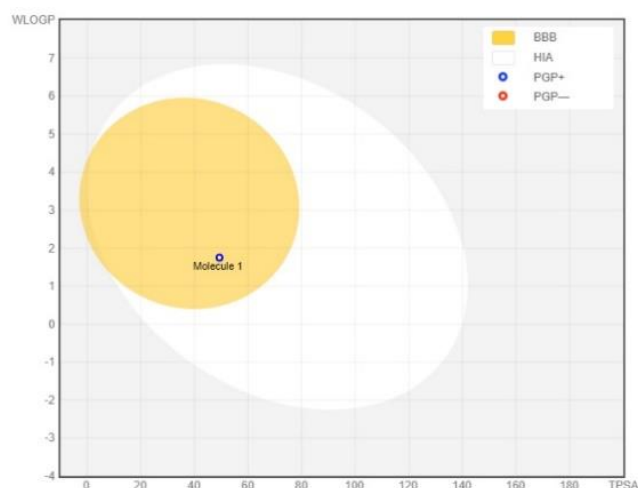


**Figure 3.** ADME properties of compound 7,12-dihydro-6H-indolo[2,3-a]acridin-13-ol (**5**) by graphical representation @ ADME (boiled-egg).

**Table 2.** Parameters obtained from molecular docking studies of AR receptors protease with compounds.

PDB ID	Autodock Result affinity (kcal/mol)	Autodock vina Result affinity (kcal/mol)
1GS4	-10.0	-10.1
1T7R	-6.9	-8.9
2AX8	-6.4	-5.4
3B66	-4.2	-6.5

AR receptor **1GS4** Compound **5** familiar one hydrogen bond (LEU704; 2.4 Å) and also favorable orientation within the AR binding site by interacting with other residues (HIS701, MET787, PHE764, LEU704, LEU873, LEU707, MET745, MET749, ALA877).

The receptor **1T7R** as against Compound **5** showed one hydrogen bonding with exhibited other kinds of interactions with various residues of AR receptor (LYS720, VAL716, MET734, VAL716, ILE737, and LYS720) presented in Figure 4.

AR receptor **2A8X** interacted through two hydrogen bonds (THR877; 2.5 and GLY708; 3.1 Å) interaction of other residues ASN705, MET787, PHE764, MET742, LEU873, MET895, MET742, MET745, VAL746, MET749. The AR receptor **3b66** also interacting with one hydrogen bond (GLN802; 1.8Å) other residues (CYS844 and PRO801) Molecular docking study of compounds suggested that several Van der Waals, covalent, carbon-hydrogen, Pi alkyl, and electrostatic interactions are the key force for bonding of **5** compound AR receptor. Compound **5** interact to supp that the AR activity of the synthesized out the compound. AR receptor **1GS4** Compound **5** binds to AR with an excellent docking score and it may be considered as an appreciable inhibitor.

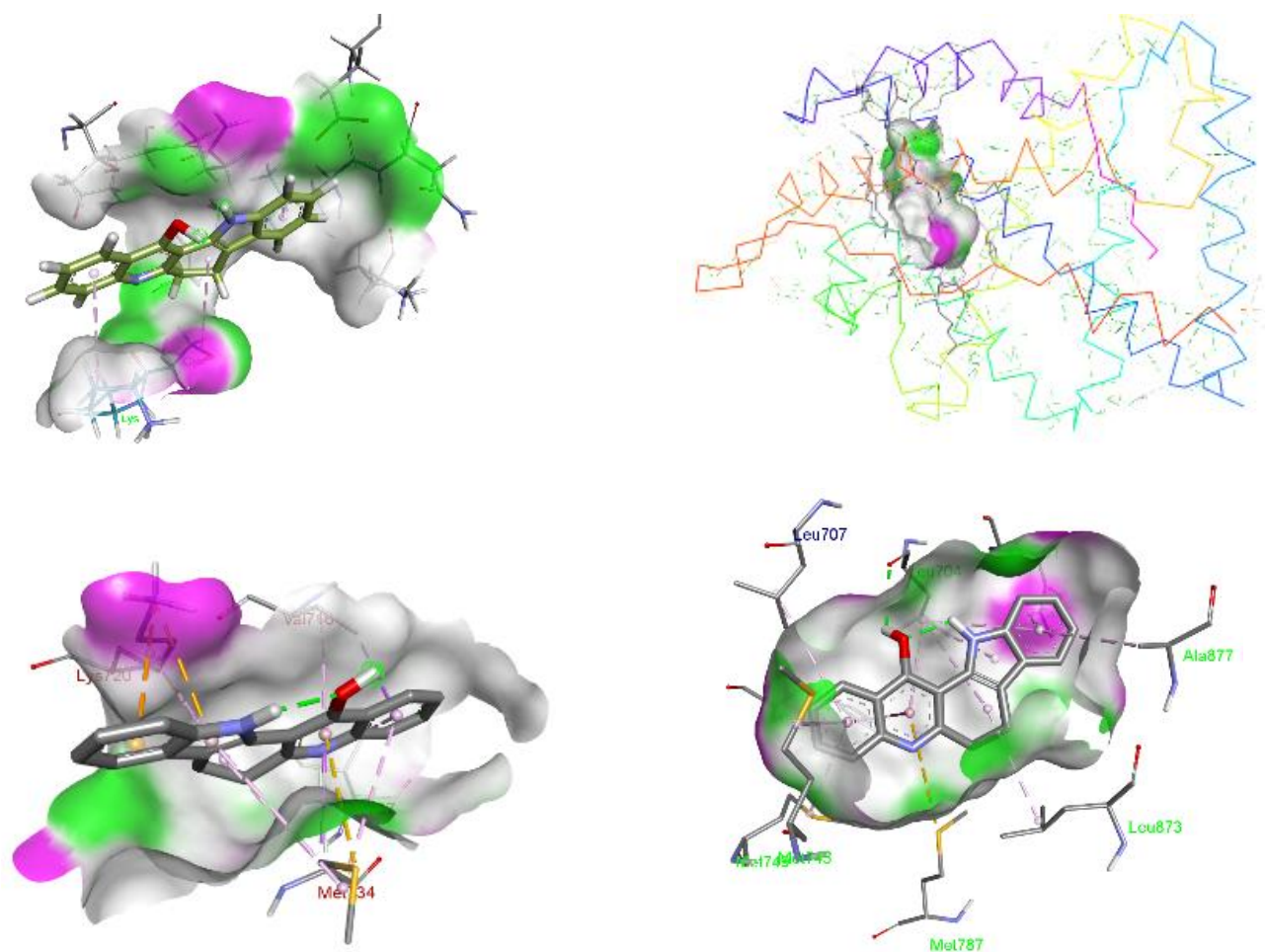


**Figure 4.** 3D Docking poses of interaction with the ligand the H-bond surfaces of the AR receptor: a) 1GS4; b) 1T7R; c) 2AX8; d) 3B66 @ Molecular docking Studies.

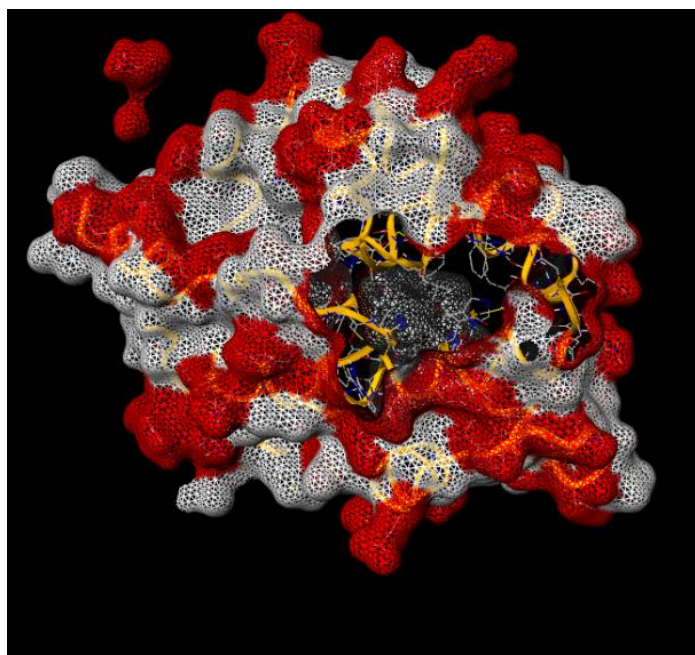


**Figure 5.** The docked ligand at the Surface area of the AR site receptor @ Molecular docking Studies.

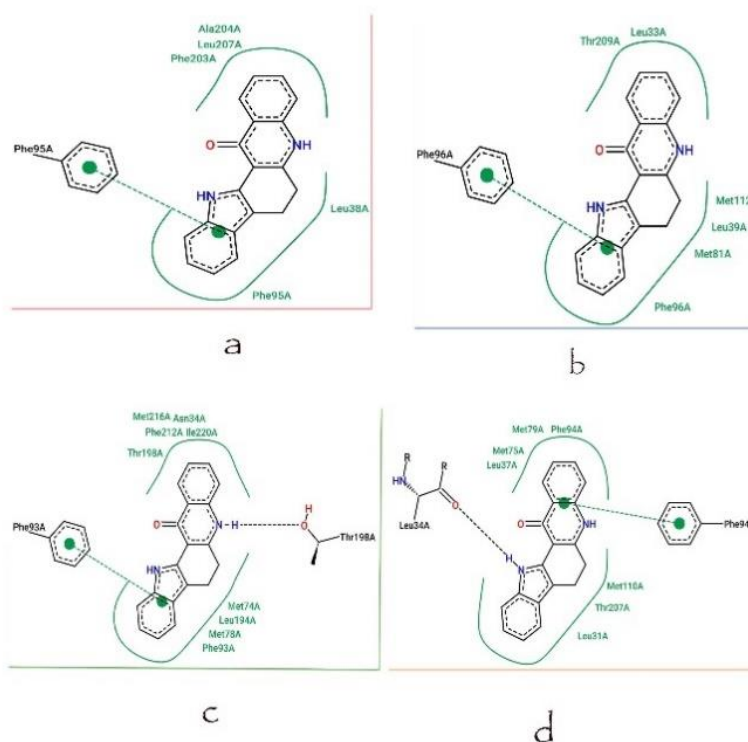


**Figure 6.** 2D Docking poses of compound **5** into the binding site of the a) 1GS4; b) 1T7R; c) 2AX8; d) 3B66 AR receptors protease @ 2D binding site.

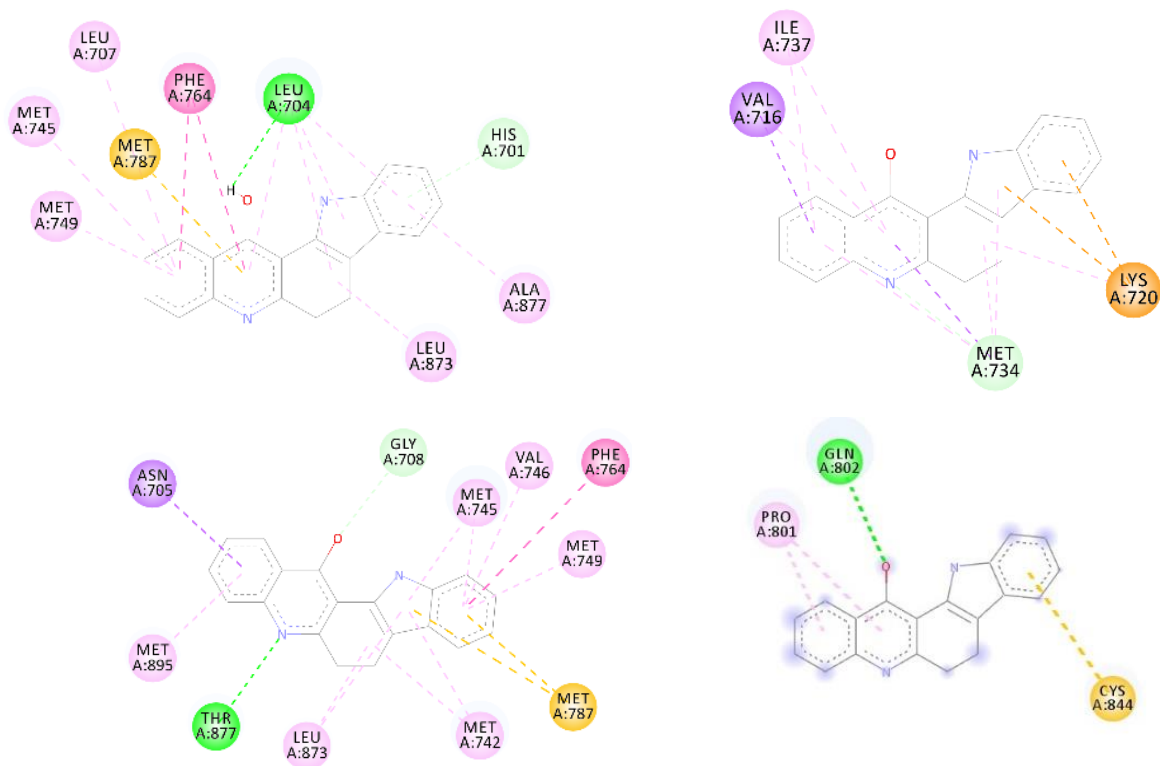


**Figure 7.** 2D interaction of the ligand **4** H-bond surfaces with a) 1GS4; b) 1T7R; c) 2AX8; d) 3B66 AR receptors protease @ 2D binding site.

## Conclusions

Molecular docking was used to design a new class of indoloacridin-13-ol AR antagonists, and the glide scores were in good agreement with the observed values. The substitution has better binding affinities, as shown by docking calculations. The reaction yielded an efficient 7,12-dihydro-6H-indolo[2,3-*a*]acridin-13-ol of potential synthetic and pharmaceutical applications, and it was carried out without the use of solvents. Compound **5** showed substantial activity against protease cancer. The compound is a potential lead for the development of selective cancer drugs, according to *in-silico* ADME reporting, toxicity, drug-likeness, drug scores results, PASS analysis, and *in vitro* results.

**Acknowledgements.** This work was supported by the Annai College of Arts and Science, Kumbakonam, VIT- University, Vellore, Tamilnadu for performing IR, NMR, GC-Mas s spectroscopy of spectral studies.

## References

1. Suzuki H., Ueda T., Ichikawa T., Ito H. *Endocr.-Relat. Cancer* **2003**, *10*, 209–216.
2. Ni M., Chen Y., Lim E., Wimberly H., Bailey S.T., Imai Y., Rimm D.L., Liu X.S., Brown M. *Cancer Cell* **2011**, *20*(1), 119–131.
3. Zelefsky M.J., Morris M.J., Eastham J.A. *Cancer of the Prostate*, Williams & Wilkins, **2019**.
4. *American cancer society*, <https://www.cancer.org/cancer/prostate-cancer/about/what-is-prostate-cancer.html> (date of access 21.07.2022).
5. Torre L.A., Bray F., Siegel R.L., Ferlay J., Lortet-Tieulent J., Jemal A. *CA Cancer J. Clin.* **2015**, *65*(2), 87–108.
6. Lacivita E., Perrone R., Margari L., Leopoldo M. *J. Med. Chem.* **2017**, *60*, 9114–9141.
7. Ali I. *Current. Can. Drug. Targets* **2011**, *11*, 131-134.
8. Haider R., Ahmad K., Siddiqui N., Ali Z., Akhtar M.J., Fuloria N., Fuloria S., Ravichandran M., Shahar Y.M. *J. Bioorg. Chem.* **2019**, *88*, 102962.
9. Rømer M.U., Nygård S.B., Christensen I.J., Nielsen S.L., Nielsen K.V., Müller S., Smith D.H., Vainer B., Nielsen H.J., Brünner N. *Mol. Oncol.* **2013**, *7*(1), 101-111.
10. Zhao B., Liu P. *Nat. Commun.* **2020**, *11*, 908.
11. Matiadis D., Sagnou M. *Int. J. Mol. Sci.* **2020**, *21*(15), 5507.
12. Wang W., Ho W.C., Dicker D.T., MacKinnon C., Winkler J.D., Marmorstein R., El-Deiry W.S. *Cancer Biotherapy* **2005**, *4*, 893-898.
13. Napolraj A., Pitchai P., Mani P. *Org. Chem. Res.* **2019**, *5*, 167-173.
14. Napolraj A., Pitchai P., Vijayarathinam M. *Malaysian J. Chem.* **2019**, *21*, 66-72.
15. Napolraj A., Shupeniuk V.I., Sathiyaseelan M., Prakash N. *Vietnam J. Chem.* **2021**, *59*, 511-521.
16. Shupeniuk V.I., Napolraj A., Tarasa T.N., Sabadakha O.P. *Russ. J. Org. Chem.* **2021**, *57*, 582-588.
17. Lipinski C.A., Lombardo F., Dominy B.W., Feeney P.J. *Adv. Drug. Deliver Rev.* **2001**, *46*, 3-26.
18. Daina A., Michielin O., Zoete V. *Sci. Rep.* **2017**, *7*, 42717.
19. Meng X.Y., Zhang H.X., Mezei M., Cui M. *Curr. Comput-Aid. Drug* **2011**, *7*, 146–157.
20. Forli S., Huev R., Pique M.E., Sanner M.F., Goodsell D.S., Olson A.J. *Nature Protocols.* **2016**, *11*, 905–919.
21. Saeed A., Ur-Rehman S., Channar P.A. *Drug. Res.* **2017**, *67*, 596–605.
22. Saeed A., Mahesar P.A., Channar P.A. *Chem. Biodivers.* **2017**, *14*, e1700035.
23. Willard L., Ranjan A., Zhang H. *Nucleic. Acids. Res.* **2003**, *31*, 3316–3319.

Received 09.02.2022

Accepted 15.04.2022